International Journal of Mass Spectrometry and Ion Processes, 81 (1987) 123–145
Elsevier Science Publishers B.V., Amsterdam – Printed in The Netherlands

SELECTED-ION FLOW TUBE STUDIES OF REACTIONS OF C_2N^+ IONS DERIVED FROM CYANOGEN BY ELECTRON IONIZATION *

DIETHARD K. BOHME, STANISŁAW WŁODEK, ASIT B. RAKSIT, HAROLD I. SCHIFF, GERVASE I. MACKAY and KAI J. KESKINEN

Department of Chemistry and Centre for Research in Experimental Space Science, York University, Downsview, Ont. M3J 1P3 (Canada)

(Received 30 April 1987)

ABSTRACT

The chemistry of C_2N^+ has been explored in a selected-ion flow tube (SIFT) apparatus in which C_2N^+ was derived by electron impact from cyanogen. Two forms of C_2N^+ were identified which have distinctly different chemical reactivities. One form appears to be the CCN^+ isomer, which reacts selectively with H_2, D_2, CO_2, Xe, and O_2. The less reactive form is thought to be the CNC^+ isomer. Reactions of both forms are also investigated with N_2, CO, HCN, C_2N_2, N_2O, H_2O, D_2O, CH_4, CH_3CN, C_2H_2, OCS, CH_3OH, C_2H_4, H_2S, NH_3, CS_2, and NO. Rate constants and product distributions are reported at 296 ± 2 K. The results exhibit a wide range in reactivity and chemistry. They provide new insight into the reactions of C_2N^+ in interstellar gas clouds and additional evidence for the formation of the CNC^+ isomer in the important interstellar reaction of C^+ with HCN.

INTRODUCTION

The C_2N^+ ion has attracted attention for its role in the chemistry of dense interstellar clouds [1,2] where it is believed to be formed from carbon cations and hydrogen cyanide according to

$$C^+ + HCN \rightarrow C_2N^+ + H \qquad (1)$$

This reaction now has been investigated in the laboratory with a range of techniques. Our own measurements using the SIFT technique [3] established that the reaction is rapid at 300 K, $k = 3.5 \times 10^{-9}$ cm^3 molecule^{-1} s^{-1}, in agreement with earlier ICR and flowing afterglow measurements [4,5].

* Dedicated to Eldon E. Ferguson in honour of his contributions in ionic physics and chemistry. Diethard K. Bohme and Harold I. Schiff have benefitted both personally and professionally from their association with Dr. Ferguson.

0168-1176/87/$03.50

Recent measurements with the variable-temperature SIFT technique have shown that the specific rate for this reaction has a slight negative temperature dependence proceeding with an efficiency of more than 60% in the temperature range from 205 to 540 K [6].

Haese and Woods [7] were the first to question the structure of the C_2N^+ ion produced in reaction (1). The structures CCN^+ and CNC^+ were proposed as possibilities and ab initio calculations were reported for the heats of formation of the two isomers and the barrier for isomerization between them [7]. The results of these calculations, together with available appearance potential measurements, indicated to Haese and Woods that reaction (1) may selectively produce the CNC^+ isomer, but no direct experimental data were available at the time to support this prediction.

The theoretical prediction of two structural isomers of C_2N^+ has found support from several experimental studies of C_2N^+ ion formation by electron impact on C_2N_2, CH_3CN, CH_3NC, and HC_3N [8,9]. These have identified two states of C_2N^+ with different enthalpies of formation, viz. 387.2 ± 3.6 and 412.5 ± 3.6 kcal mol^{-1}. These two states are likely to correspond to the CNC^+ and CCN^+ isomer, respectively. The experimental energy difference of 25.3 kcal mol^{-1} is considerably lower than the earlier prediction of 48.7 kcal mol^{-1} for the isomerization energy [7], but quite consistent with the later, higher level calculations by Yoshimine and Kraemer, which led to values for the isomerization energy as low as 28.1 kcal mol^{-1} [10].

The chemical reactivity of C_2N^+ has now also been explored in several laboratory studies and for several different sources of C_2N^+. The reactivity of C_2N^+ ions produced chemically by reaction (1) has been probed in an earlier SIFT study in our own laboratory [11]. There has also been an ICR study of the reactivity of C_2N^+ at near thermal energies in which the C_2N^+ was produced by electron impact on C_2N_2 at close to the appearance energy [12]. The C_2N^+ in these latter experiments was thought to be the higher energy CCN^+ isomer, in part because of a few apparent differences in product distributions between the ICR results and the earlier SIFT results [11].

In the meantime, there has also been a report of a crossed ion beam–molecular beam study of reaction (1) at relative energies between 0.62 and 1.57 eV [13]. The kinetic energy release observed in these experiments indicated a large exothermicity for this reaction which is consistent only with the production of the more stable CNC^+ isomer.

In the SIFT experiments reported here, a mixture of two states of C_2N^+ is produced by electron ionization of cyanogen at electron energies well above the appearance energies of both isomers. Two components of C_2N^+ are identified on the basis of distinctly different reactivities with a number of

specific gases. Considerations of the thermochemistry of some of the observed reactions of the more reactive component are consistent with its identification as the CCN^+ isomer so that the less reactive component could be identified as the CNC^+ isomer. The reactivity of both components is investigated with a variety of gases and vapours chosen primarily because of their presence in interstellar clouds. Together with our earlier SIFT results for the reactivity of C_2N^+ generated by reaction (1), the results reported here provide further evidence for the production of the CNC^+ isomer in reaction (1). They also provide new insight into the state of the C_2N^+ employed in the ICR measurements reported previously [12].

EXPERIMENTAL

The measurements were performed with the selected-ion flow tube (SIFT) apparatus in the ion chemistry laboratory [14,15]. The C_2N^+ ion was generated in an axial electron impact ionizer [16] from cyanogen at electron energies in the range 50–55 eV. When C_2N^+ was injected upstream, the major impurity ions observed downstream were CH_2N^+ and CHO^+, which arise from reactions with the water vapour impurity in the helium buffer gas. Lesser impurity ions present were C_2NO^+, which may arise from the reaction of the high-energy form of C_2N^+ with oxygen impurity, H_3O^+ which is produced from CHO^+ and water vapour, and C^+ which results from collisional dissociation of the C_2N^+. The C_2N^+ ions were injected into helium buffer gas at laboratory energies of ca. 10–50 V. The total pressure in the reaction region was in the range 0.32–0.35 torr and the ambient temperature was 296 ± 2 K. The reactant gases and vapours, as well as the helium buffer gas, were generally of high purity, with a minimum purity of 99.5 mol.%. Hydrogen cyanide was prepared according to the procedure described by Glemser [17].

RESULTS AND DISCUSSION

In the course of the survey of the reactions reported in this study, it became evident with several reactants that the C_2N^+ ions derived from C_2N_2 had two components of different reactivity. This was especially the case with hydrogen, deuterium, carbon dioxide, oxygen, and xenon for which there was one component of C_2N^+ which was very reactive and another component which was essentially unreactive. With some gases, both components were reactive but they had different reactivities. In still other cases, both components were equally reactive or equally unreactive. The data obtained with two components present with different reactivities were analysed according to the methods described by Glosik et al. [18]. About

25% of the C_2N^+ ions generated from cyanogen at the electron energies employed in this study was found to be in the more reactive state. Results obtained for the reactions of this state are summarized in Table 1.

TABLE 1

Rate constants (in units of 10^{-9} cm^3 molecule^{-1} s^{-1}) and product distributions for selected reactions of the more reactive component of C_2N^+, presumably CCN^+, measured with the SIFT technique at 296 ± 2 K [a]

Neutral reactant	Products	Branching ratio [b]	k_{exp} [c]	k_c [d]
N_2	$C_2N_3^+$	1.0	≤ 0.0001	0.77
H_2	$CH_2N^+ + C$	0.95	0.3	1.5
	$C_2H_2N^+$	0.05		
CO	C_3NO^+	1.0	≤ 0.0005	0.85
HCN	$C_3HN_2^+$	1.0	0.29	3.5
CO_2	$C_2NO^+ + CO$	0.8	1.0	0.84
	$C_3O^+ + NO$	0.2		
C_2N_2	$C_4N_3^+$	1.0	0.15	1.1
N_2O	$C_2NO^+ (CN_3^+) + N_2(CO)$	0.9	0.53	0.93
	$NO^+ + C_2N_2$	0.1		
H_2O	$CHO^+ + CHN$	0.5	1.0	2.6
	$C_2NO^+ + H_2$	0.3		
	$CH_2N^+ + CO$	0.2		
CH_4	products		0.35	1.1
CH_3CN	$C_2H_3^+ + C_2N_2$	0.9	3.1	4.1
	$C_2N_2H^+ + C_2H_2$	0.1		
Xe	$Xe^+ + C_2N$	1.0	0.03	0.87
O_2	$C_2NO^+ + O$	1.0	0.3	0.71
C_2H_2	$C_3H^+ + CHN$	0.8	1.0	1.1
	$CH_2N^+ + C_3$	0.2		
OCS	$C_2NO^+ + CS$	1.0	0.95	1.3
CH_3OH	products		2.1	2.2
C_2H_4	products		1.0	1.2
H_2S	products		1.2	1.5
NH_3	products		1.8	2.3
CS_2	products		0.92	1.3
NO	$NO^+ + C_2N$	1.0	0.62	0.79

[a] The C_2N^+ ions were derived from C_2N_2 by electron impact at ca. 50 eV.

[b] Primary product ions which contribute 5% or more. The product distributions have been rounded off to the nearest 5% and are estimated to be accurate to $\pm 30\%$. See text for details about products not specified.

[c] The apparent bimolecular rate constant is given in each case. All measurements were made in helium buffer gas at at total pressure of ca. 0.34 torr and a number density of 1.1×10^{16} atoms cm^{-3}. The accuracy is estimated to be $\pm 50\%$.

[d] Collision rate constants are derived from the combined variational transition state theory–classical trajectory study of Su and Chesnavich [29].

TABLE 2

Summary of rate constants (in units of 10^{-9} cm^3 $molecule^{-1}$ s^{-1}) and product distributions for reactions of the less reactive component of C_2N^+, presumably CNC^+, measured with the SIFT technique at 296 ± 2 K [a]

Neutral reactant	Products	Branching ratio [b]	k_{exp} [c]	k_c [d]
N_2	$C_2N_3^+$	1.0	≤ 0.0001	0.77
H_2			≤ 0.0001	1.5
CO	C_3NO^+	1.0	≤ 0.0005	0.85
HCN	$C_3HN_2^+$	1.0	0.29	3.5
CO_2			≤ 0.00003	0.84
C_2N_2	$C_4N_3^+$	1.0	0.15	1.1
N_2O	$C_2NO^+(CN_3^+)+N_2(CO)$	0.9	0.53	0.93
	$NO^+ + C_2N_2$	0.1		
H_2O	$CHO^+ + CHN$	0.7	0.11	2.6
	$CH_2N^+ + CO$	0.3		
CH_4	$C_2H_3^+ + CHN$	0.7	0.0039	1.1
	$C_3H_2N^+ + H_2$	0.2		
	$CH_2N^+ + C_2H_2$	0.1		
CH_3CN	$C_2H_3^+ + C_2N_2$	1	3.1	4.1
Xe			≤ 0.0005	0.87
O_2			≤ 0.0001	0.71
C_2H_2	$C_3H^+ + CHN$	0.8	1.0	1.1
	$CH_2N^+ + C_3$	0.2		
OCS	$C_2NS^+ + CO$	1	0.95	1.3
CH_3OH	$CH_3^+ + C_2HNO$	0.3	2.1	2.2
	$C_2H_3O^+(CHNO^+)+CHN(C_2H_3)$	0.3		
	$CH_3O^+(HNO^+)+C_2HN(C_3H_3)$	0.1		
	$C_2H_2N^+ + CH_2O$	0.1		
	$C_3H_2N^+ + H_2O$	0.1		
	$C_2NO^+(C_3H_4N^+)+CH_4(O)$	0.1		
C_2H_4	$C_3H_3^+ + CHN$	0.5	1.0	1.2
	$C_2H_2N^+ + C_2H_2$	0.25		
	$C_4H_2N^+ + H_2$	0.15		
	$C_2H_4^+ + C_2N$	0.1		
H_2S	$CHS^+ + CHN$	0.95	1.2	1.5
	$C_2NS^+ + H_2$	0.05		
NH_3	$CH_2N^+ + CHN$	1	1.8	2.3
CS_2	$C_2NS^+ + CS$	1.0	0.92	1.3
NO	$NO^+ + C_2N$	1.0	0.62	0.79

[a] The C_2N^+ ions were derived from C_2N_2 by electron impact at ca. 50 eV. Oxygen was added upstream to scavenge the more reactive component of C_2N^+.

[b] Primary product ions which contribute 5% or more to the total product ions. Product distributions have been rounded off to the nearest 5%.

[c] The apparent bimolecular rate constant is given in each case. All measurements were made in helium buffer gas at a total pressure of ca. 0.34 torr and a number density of 1.1×10^{16} atoms cm^{-3}. The accuracy is estimated to be ±30%.

[d] Collision rate constants are derived with the combined variational transition state theory–classical trajectory study of Su and Chesnavich [29].

The observed selective reactivity of the more reactive component was exploited by deliberately adding an appropriate reactive gas upstream of the reaction region to remove or scavenge the more reactive component. In most experiments, oxygen was chosen as the scavenger gas, but hydrogen and deuterium were also used occasionally. Table 2 summarizes the rate constants and product distributions determined for reactions of C_2N^+ ions after scavenging the more reactive state with oxygen (unless indicated otherwise). Rate constants and product distributions under these conditions were derived in the usual manner [15,19].

Both Tables 1 and 2 include all the primary product ions which were observed to contribute 5% or more to the total products. The reactants are listed in order of decreasing ionization energy of the neutral substrate. All rate constants are reported as effectively bimolecular. Unless indicated otherwise, the measurements were made at a total pressure of 0.34 torr and a helium number density of 1.1×10^{16} atoms cm^{-3}.

N_2

No measurable reaction was observed between C_2N^+ and nitrogen in the absence or presence of scavenger gas, $k \leq 1 \times 10^{-13}$ cm^3 $molecule^{-1}$ s^{-1}, although traces of an ion with a mass equal to that of the adduct ion $C_2N_3^+$ were observed to be formed. C_2NO^+, which was present when oxygen was added upstream, was found to be equally unreactive.

Previous ICR measurements also indicated no reaction between C_2N^+ and nitrogen, $k \leq 1 \times 10^{-11}$ cm^3 $molecule^{-1}$ s^{-1} [12].

H_2, D_2

Reactive and non-reactive components of C_2N^+ were evident with H_2 and D_2. With hydrogen, the reactive component was observed to produce CH_2N^+ and some $C_2H_2N^+$ rapidly, $k = (3 \pm 1) \times 10^{-10}$ cm^3 $molecule^{-1}$ s^{-1}. Experiments with D_2, which avoided complications introduced by an initial signal at $m/z = 28$, provided a branching ratio of 16 to 1. For the rate constants of the non-reactions of C_2NO^+, O_2^+, and the non-reactive component of C_2N^+, we can report upper limits of 1×10^{-13} cm^3 $molecule^{-1}$ s^{-1}.

The diverse reactivity towards hydrogen exhibited by the two forms of C_2N^+ can be understood in terms of the presence of CCN^+ and CNC^+ isomers. The available thermochemical information for these two isomers, and for the possible isomers of the CH_2N^+ ion which is produced, indicate that only the higher energy CCN^+ isomer can form CH_2N^+ and that this latter ion must be the lowest-energy CH_2N^+ isomer, viz. nitrogen-protonated HCN, as indicated in the reaction

$$CCN^+ + H_2 \rightarrow HCNH^+ + C \qquad (2)$$

This implies that the reactive component of the C_2N^+ generated in this study is CCN^+ and that the non-reactive component is CNC^+. The reaction is likely to proceed by H–H bond insertion followed by a 1,2 H-atom shift and proton transfer as indicated in the reaction

$$CCN^+ + H_2 \rightarrow [CH_2^+\text{–}CN] \rightarrow [CH^+ \cdots HCN] \rightarrow C + HCNH^+ \quad (3)$$

A small fraction of the adduct ion seems to be stabilized by collision with the helium buffer gas and appears as a minor channel.

CO

A small but definite decay was observed for the C_2N^+ ion when CO was added into the reaction region. The apparent bimolecular rate constant was $k \leq 5 \times 10^{-13}$ cm^3 molecule^{-1} s^{-1}. The adduct ion C_3NO^+ was observed to be formed both in the presence and absence of O_2. However, the decay in the C_2N^+ signal was too shallow to allow the determination of a reliable absolute rate constant for the reaction of either form of the C_2N^+. No adducts or decays were observed for the C_2NO^+ and O_2^+ ions. We can report here an upper limit of 1×10^{-13} cm^3 molecule^{-1} s^{-1} for the specific rates of the non-reactions of these latter two ions.

The C_3NO^+ ion derived from CO addition was not detected in the ICR measurements and an upper limit of only 1.0×10^{-11} cm^3 molecule^{-1} s^{-1} was reported for the specific reaction rate [12]. The small apparent bimolecular rate constant for the addition reaction observed in our SIFT experiments is suggestive of the formation of a weakly bound adduct of the type $C_2N^+ \cdot CO$ in which only electrostatic forces contribute to the bonding.

HCN

No difference was observed in the C_2N^+ decay and the nature of the products with and without oxygen. Both forms of C_2N^+ appeared to add one molecule of HCN according to

$$C_2N^+ + HCN \rightarrow C_3HN_2^+ \quad (4)$$

The measured apparent bimolecular rate constant was 2.9×10^{-10} cm^3 molecule^{-1} s^{-1}, which corresponds to about 10% of the collisional rate constant. Further sequential additions of HCN were observed with formation up to $C_2N^+ \cdot (HCN)_4$. The C_2NO^+ produced in the presence of oxygen was found to be unreactive towards HCN, $k \leq 2 \times 10^{-12}$ cm^3 molecule^{-1} s^{-1}.

The rate constant obtained for reaction (4) agrees with the value of 3.1×10^{-10} cm^3 molecule^{-1} s^{-1} determined previously in a flowing after-

glow study in which the products were not identified [20]. The previous ICR study at much lower pressures [12] showed no reaction, $k \leq 3 \times 10^{-11}$ cm^3 molecule^{-1} s^{-1}, as would be expected if reaction (4) proceeds in a termolecular fashion. The high apparent bimolecular rate constant is suggestive of chemical bonding in the formation of the adduct, as would be the case, for example, if the addition proceeds by C–H bond insertion to form NC–CH^+–CN (with CCN^+) or :C=N–CH^+–CN (with CNC^+) [21]. Loss of a proton from the latter two ions should generate the neutral carbenes $:C(CN)_2$ and :C(NC:)CN, respectively.

CO_2

Two components of C_2N^+ were clearly evident from the measurements of the C_2N^+ decay with added carbon dioxide. Representative data are shown in Fig. 1. One component was totally unreactive, $k \leq 3 \times 10^{-14}$ cm^3 molecule^{-1} s^{-1}. In sharp contrast, the reactive component produced products at near the collision rate, $k = 1.0 \times 10^{-9}$ cm^3 molecule^{-1} s^{-1}. These results can be understood again in terms of two isomers of C_2N^+. Available thermochemical information indicates that only the CCN^+ isomer can produce C_3O^+. This again implies that the reactive component is CCN^+ and the unreactive component is CNC^+. The observed reactions with the reactive C_2N^+ species were

$$CCN^+ + CO_2 \xrightarrow{0.8} C_2NO^+ + CO \quad (5a)$$

$$\xrightarrow{0.2} C_3O^+ + NO \quad (5b)$$

The C_2NO^+ and C_3O^+ were both unreactive towards CO_2, $k \leq 10^{-12}$ cm^3 molecule^{-1} s^{-1}. The mechanism for channel (5b) is intriguing since it must involve the cleavage of the C–N bond in C_2N^+. One plausible route involves an intermediate intramolecular reaction of the type shown in (6) in which the $CCNO^+$ isomer is formed initially by O-atom abstraction.

$$:CCN^+ + O{=}C{=}O \rightarrow [:C{=}C^+{-}N{=}O + :CO] \rightarrow [OC: + :C{=}C^+{-}N{=}O]$$
$$\rightarrow O{=}C{=}C{=}C^{+\cdot} + {\cdot}N{=}O \quad (6)$$

The previous ICR study indicated no reaction with CO_2, $k \leq 1 \times 10^{-11}$ cm^3 molecule^{-1} s^{-1} [12]. In view of our SIFT results, this non-reactivity implies that the C_2N^+ ion generated in the ICR study was predominantly the CNC^+ isomer.

C_2N_2

We have previously reported the observation of a rapid addition reaction of C_2N^+ with C_2N_2 with an apparent bimolecular rate constant of 1.5×10^{-10}

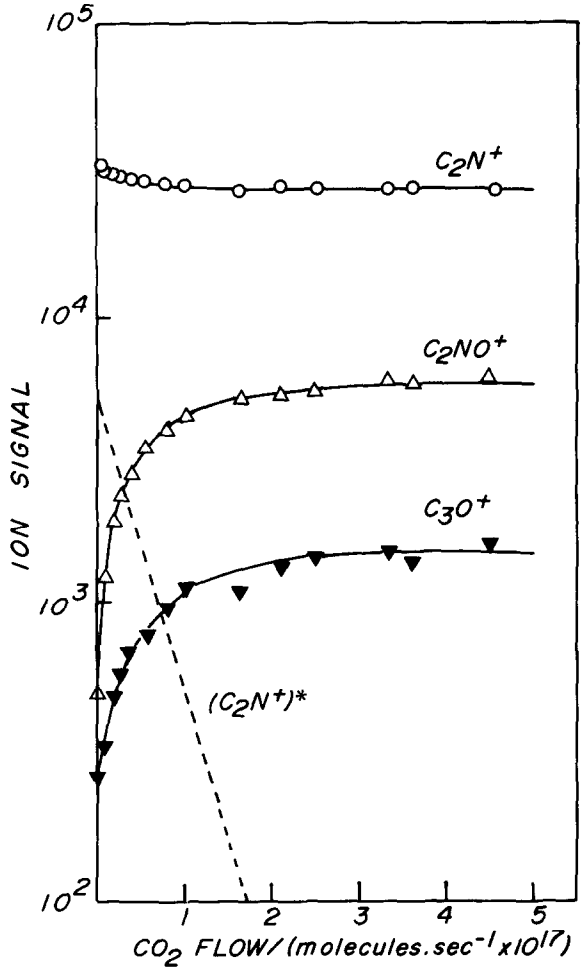

Fig. 1. Observations of the reactivity of two components of C_2N^+ towards carbon dioxide added into the reaction region of the SIFT apparatus in which C_2N^+ is initially established as the dominant ion. The buffer gas is helium. $P = 0.34$ torr, $\bar{v} = 6.7 \times 10^3$ cm s^{-1}, $L = 46$ cm, and $T = 296$ K. The C_2N^+ is derived from cyanogen at 52 eV. The broken curve represents the contribution of the reactive component of C_2N^+ to the decay of C_2N^+.

cm^3 molecule^{-1} s^{-1} in helium buffer gas at 0.33 torr [22]. The C_2N^+ in these earlier experiments was generated from cyanogen at 45 eV. A similar result was obtained in the study reported here with electron ionization energies up to 10 eV higher. Addition of oxygen upstream did not alter the decay of the C_2N^+ signal. The product $C_2N^+ \cdot C_2N_2$ ion, however, appeared to react with the oxygen to establish C_2NO^+ by the reaction

$$C_4N_3^+ + O_2 \rightarrow C_2NO^+ + (C_2N_2O) \qquad (7)$$

The neutral product was not identified but may be the cyanate N ≡ C–O–C ≡ N or isocyanate N ≡ C–N=C=O. The C_2NO^+ did not react further with cyanogen, $k \leq 2 \times 10^{-12}$ cm^3 molecule^{-1} s^{-1}.

The high rates of association with the non-polar cyanogen molecule observed with the two components of C_2N^+ suggest the formation of stable adduct ions such as $^+C(CN)_3$ (from CCN^+) and $^+C(N{=}C{:})(CN)_2$ which could result from C–C bond insertion.

N_2O

Both forms of C_2N^+ reacted with nitrous oxide. The addition of oxygen upstream did not appear to alter the slope of the observed C_2N^+ decay or the distribution of the two major product ions. The reactions which were occurring appeared to be

$$C_2N^+ + N_2O \xrightarrow{0.9} C_2NO^+ + N_2 \quad (8a)$$

$$\xrightarrow{0.1} NO^+ + C_2N_2 \quad (8b)$$

The product ion at $m/z = 54$ was taken to be C_2NO^+ rather than CN_3^+, which is also allowed stoichiometrically. The mechanism for O-atom abstraction seems more likely than N_2 abstraction to form CN_3^+ and CO, particularly in view of the occurrence of nitride ion abstraction to produce C_2N_2 and NO^+. There were no observable secondary reactions with N_2O for the N_2O additions employed, $k \leq 2 \times 10^{-12}$ cm^3 molecule^{-1} s^{-1}.

H_2O, D_2O

Two states appeared to contribute to the observed decay of C_2N^+ with the addition of water vapour into the reaction region. A rate constant of 1.0×10^{-9} cm^3 molecule^{-1} s^{-1} was determined for the reaction of the more reactive component from the initial curvature in the semi-logarithmic decay. The rate constant for the less reactive component was determined from the final slope in the semi-logarithmic decay and from the decay observed when oxygen or deuterium was added as the scavenger gas upstream. It was found to be 1.1×10^{-10} and 8.2×10^{-11} cm^3 molecule^{-1} s^{-1} for H_2O and D_2O, respectively.

Experiments with H_2O and D_2O as the reactants, with and without the addition of oxygen scavenger gas upstream, indicated the major products of the less reactive component to be CHO^+ (CDO^+) and CH_2N^+ (CD_2N^+). The ions C_2HN^+ and $C_2H_2N^+$ were identified as minor products with branching ratios of less than 5%. The C_2NO^+ ion was shown to be produced exclusively by the more reactive component in experiments with and without

deuterium as a scavenger gas. An analysis of the products in the absence of scavenger gas, at low additions of H_2O at which the reaction of the more reactive component should dominate, indicated the product distribution

$$CCN^+ + H_2O \xrightarrow{0.5} CHO^+ + CHN \quad (9a)$$

$$\xrightarrow{0.3} C_2NO^+ + H_2 \quad (9b)$$

$$\xrightarrow{0.2} CH_2N^+ + CO \quad (9c)$$

The product distribution reported for the ICR experiments is different [12]. It does not match the distribution observed in the SIFT experiments for either component of C_2N^+. CHO^+ was observed to be the main product ion (75%) but C_2HN^+ was observed to contribute 25% to the product spectrum, while CH_2N^+ was not reported as a product, nor was C_2NO^+. The ICR rate constant of 3.4×10^{-10} cm^3 molecule^{-1} s^{-1} is closer to that determined in the SIFT experiments for the lower energy component.

The CHO^+ and CH_2N^+ are likely to arise from O–H bond insertion without and with subsequent intramolecular proton transfer before separation of the products.

CH_4

Curvature in the C_2N^+ decay was also observed with the addition of methane and again indicated the presence of two components of different reactivity. Small additions led to a rapid rise in ions at $m/z = 27$, 52, and 28. The 27 ion was identified as $C_2H_3^+$ rather than HCN^+ because of its further reaction with CH_4 to form $C_3H_5^+$. The 52 ion must be $C_3H_2N^+$ and 28 may be CH_2N^+ or $C_2H_4^+$. Production of $C_2H_4^+$ was ruled out with CD_4. Further production of these ions appeared to occur also at higher additions of methane where the decay of C_2N^+ followed a rate constant of 3.9×10^{-12} cm^3 molecule^{-1} s^{-1}. Analysis of the initial strong curvature in the early decay yielded a rate constant of 3.5×10^{-10} cm^3 molecule^{-1} s^{-1} for the reaction of the more reactive component. In the experiments in which oxygen was added, the O_2^+ was observed to react with methane in the known fashion to produce $CH_3O_2^+$ [23], while C_2NO^+ appeared unreactive towards methane, $k \leq 1 \times 10^{-13}$ cm^3 molecule^{-1} s^{-1}. An upper limit of 1×10^{-11} cm^3 molecule^{-1} s^{-1} was obtained in the ICR experiments for the rate constant of the reaction of C_2N^+ with methane. Again, this result is more consistent with the presence of the lower energy CNC^+ isomer in the ICR experiments.

Formation of the $C_2H_3^+$ and CH_2N^+ products can be understood in terms of C–H bond insertion without and with subsequent intramolecular

proton transfer before separation of the products. Abstraction of methylene from methane could lead to the formation of the $C_3H_2N^+$, which could be either $N \equiv C-C^+=CH_2$ (formed from CCN^+) or $:C=N-C^+=CH_2$ (formed from CNC^+).

CH_3CN

No difference was observed in the decay of C_2N^+ in the presence or absence of oxygen scavenger gas. The predominant product observed was $C_2H_3^+$, which was distinguished from HCN^+ through experiments with CD_3CN. A second product was $C_2N_2H^+$ but it was minor. The two observed reaction channels are

$$C_2N^+ + CH_3CN \rightarrow C_2H_3^+ + C_2N_2 \quad (10a)$$

$$\rightarrow C_2N_2H^+ + C_2H_2 \quad (10b)$$

In the presence of oxygen, the latter channel contributed less than 5% to the total products. When the oxygen was shut off, this contribution increased to approximately 10%. Apparently more of the CCN^+ isomer produces the $C_2N_2H^+$ product. The latter may arise by proton transfer from $C_2H_3^+$ within the collision complex before the products completely separate.

Both the ions C_2NO^+ and O_2^+, formed when O_2 was added upstream, reacted further with CH_3CN. The product ions were uncertain, but some adduct ions were observed to be formed. The known secondary proton transfer reactions with $C_2H_3^+$ and $C_2N_2H^+$ and the addition reaction of the resulting CH_3CNH^+ with CH_3CN were also observed.

Xe

With Xe as the reactant, two components of C_2N^+ were again evident. The reactive component was observed to produce Xe^+ by the charge transfer reaction

$$CCN^+ + Xe \rightarrow Xe^+ + C_2N \quad (11)$$

Analysis of the initial decay of C_2N^+ provided a rate constant of $3 \pm 2 \times 10^{-11}$ cm^3 molecule^{-1} s^{-1} for this reaction. For the unreactive component, we can report an upper limit to the rate constant of 5×10^{-13} cm^3 molecule^{-1} s^{-1}.

O_2

Addition of oxygen to the helium buffer gas in which C_2N^+ was established as the predominant ion indicated two components of C_2N^+ with

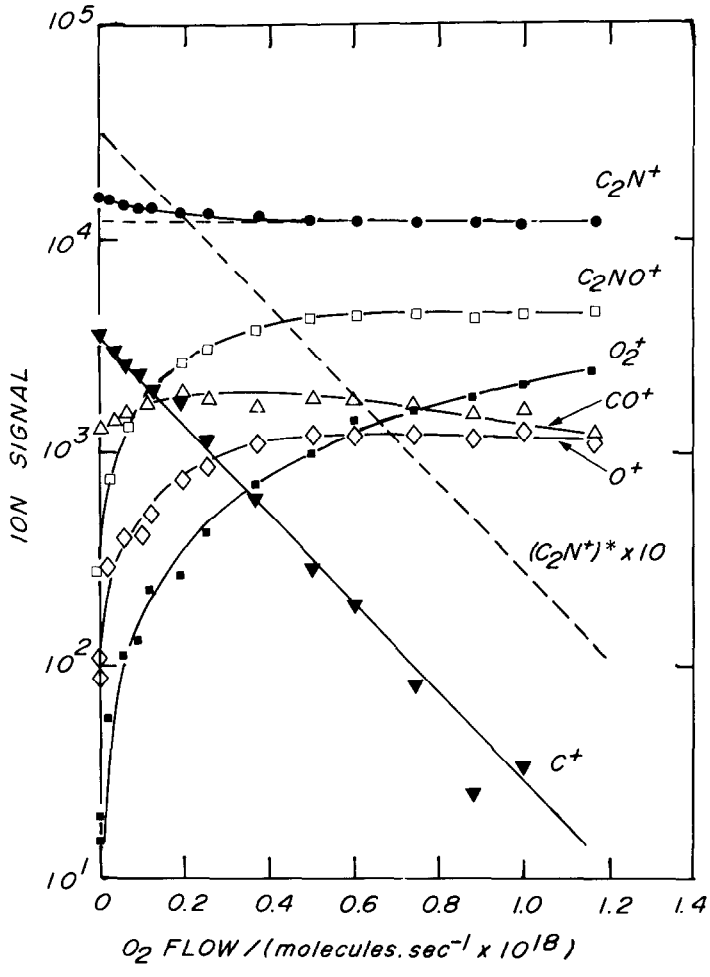

Fig. 2. Observations of the reactivity of two components of C_2N^+ towards oxygen added into the reaction region of the SIFT apparatus in which C_2N^+ is initially established as the dominant ion. The buffer gas is helium. $P = 0.35$ torr, $\bar{v} = 6.5 \times 10^3$ cm s^{-1}, $L = 46$ cm, and $T = 295$ K. The C_2N^+ is derived from cyanogen at 54 eV. The broken curve represents the contribution of the reactive component of C_2N^+ to the decay of C_2N^+. The residual chemistry initiated by C^+ leads to CO^+ and O^+ and then O_2^+.

distinctly different reactivities. About 75% of the C_2N^+ was unreactive towards oxygen, $k \leq 1.4 \times 10^{-13}$ cm^3 molecule^{-1} s^{-1}. The remaining 25% responded to the oxygen in the manner indicated by

$$CCN^+ + O_2 \rightarrow C_2NO^+ + O \qquad (12)$$

Results are shown in Fig. 2. Analysis of the initial decay of the C_2N^+ ion provided a rate constant of $(3 \pm 1) \times 10^{-10}$ cm^3 molecule^{-1} s^{-1} for the reactive component which should be the CCN^+ isomer.

C_2NO^+ was observed to be quite unreactive towards oxygen, $k \leq 1 \times 10^{-13}$ cm^3 molecule^{-1} s^{-1}.

C_2H_2

A rapid reaction was observed with acetylene both in the absence and presence of oxygen, $k = 1.0 \times 10^{-9}$ cm^3 molecule^{-1} s^{-1}. The predominant product ion was C_3H^+, which reacted further with acetylene to produce $C_5H_3^+$ and $C_5H_2^+$ [14]. Some formation of CH_2N^+ was also evident. The measured product distribution in the presence of oxygen is indicated in the reaction

$$C_2N^+ + C_2H_2 \xrightarrow{0.8} C_3H^+ + HCN \quad (13a)$$

$$\xrightarrow{0.2} CH_2N^+ + C_3 \quad (13b)$$

It did not alter significantly when the oxygen was removed. Traces (up to 5%) of HCN^+ also appeared to be produced. The O_2^+ ion formed in the presence of oxygen was observed to react with acetylene while the C_2NO^+ ion was unreactive, $k \leq 2 \times 10^{-12}$ cm^3 molecule^{-1} s^{-1}.

The ICR measurements of the reaction of C_2N^+ with acetylene also led to a rate constant of 1.0×10^{-9} cm^3 molecule^{-1} s^{-1} but a different product distribution [12]. 80% of the reaction was reported to lead to C_3H^+ while the remaining 20% was attributed to formation of HC_4N^+. In our SIFT experiments, the formation of the ion at $m/z = 63$ was shown by the product analysis to be due entirely to the secondary reaction between C_3H^+ and C_2H_2. The assignment of HC_4N^+ was reported to be confirmed in the ICR experiments with measurements involving C_2D_2. Such confirmation would only be possible if account were taken of the $C_4D_2^+$ ion formed from C_3D^+ and C_2D_2.

The two channels of reaction (13) are related by proton transfer. The reaction is likely to be initiated by C–H bond insertion which can lead to the formation of C_3H^+ and CHN. The transfer of a proton before these products completely separate will produce CH_2N^+ and the C_3 molecule.

OCS

Again, a rapid reaction was observed both in the absence and presence of O_2, $k = 9.5 \times 10^{-10}$ cm^3 molecule^{-1} s^{-1}. The product ion spectrum in the absence of oxygen contained mainly C_2NS^+ (80%) and C_2NO^+ (20%) with minor amounts of OCS^+ ($\leq 3\%$). Production of C_2NO^+ is difficult to detect in the presence of oxygen because of its relatively large initial signal but no C_2NO^+ appeared to be produced under these conditions. Experiments in

hydrogen buffer gas showed no production of C_2NO^+. These results indicate that the predominant reaction with the CNC^+ isomer is S-atom abstraction, while that with the CCN^+ isomer is O-atom abstraction.

The C_2NS^+ and C_2NO^+ ions did not react further with OCS, $k \leq 2 \times 10^{-12}$ cm^3 molecule^{-1} s^{-1}, while the O_2^+ was observed to react with OCS by charge transfer.

CH_3OH

C_2N^+ was observed to react rapidly with methanol, $k = 2.1 \times 10^{-9}$ cm^3 molecule^{-1} s^{-1}, both in the absence and presence of oxygen. Many product ions appeared to be formed with CH_3^+ (NH^+) and CH_3CO^+ ($CHNO^+$) being dominant. The product analysis was complicated by the large number of products and their secondary reactions and the reaction of O_2^+ with methanol. The $m/z = 15$ product ion was observed to react further with methanol to form the adduct and so could be identified as CH_3^+ rather than NH^+, which would be expected to proton transfer. Other product ions observed were CH_3O^+ (HNO^+), $C_2H_2N^+$, $C_3H_2N^+$ and C_2NO^+ ($C_3H_4N^+$), and some CH_4O^+ (H_2NO^+) when the oxygen was removed. The products in parentheses are allowed by stoichiometry, but are all unlikely in view of the expected mechanisms of the reactions as well as the relative stability of the concomitant neutral products.

Reasonable mechanisms can be envisaged for all six of the observed products. CH_3O^+ will result from hydride ion transfer and C_2NO^+ from oxygen atom transfer. Formation of CH_3^+ may occur from C–O bond insertion. The concomitant neutral product is likely to be the carbene :C(CN)OH in the case of CCN^+ and :C(NC)OH in the case of CNC^+. O–H bond insertion with intramolecular proton transfer can explain the $C_2H_2N^+$ product ion. C–H bond insertion provides pathways towards formation of $C_2H_3O^+$ and $C_3H_2N^+$.

C_2H_4

Four primary products were identified for the reaction of C_2N^+ with ethylene, viz. $C_3H_3^+$, $C_2H_2N^+$, $C_4H_2N^+$, and $C_2H_4^+$. The product distribution and primary ion decay were not significantly influenced by the presence of oxygen or deuterium scavenger gas. Table 2 provides the product distribution determined in the presence of scavenger gas for the reaction with the lower-energy CNC^+ isomer. It is based on analyses of the type shown in Fig. 3. The reactivity of the $C_3H_3^+$ product ion which is evident from Fig. 3 suggests that about 70% of this ion is the propargyl cation. This isomer is known to react rapidly with C_2H_4 to produce $C_5H_5^+$ and $C_5H_7^+$ [24].

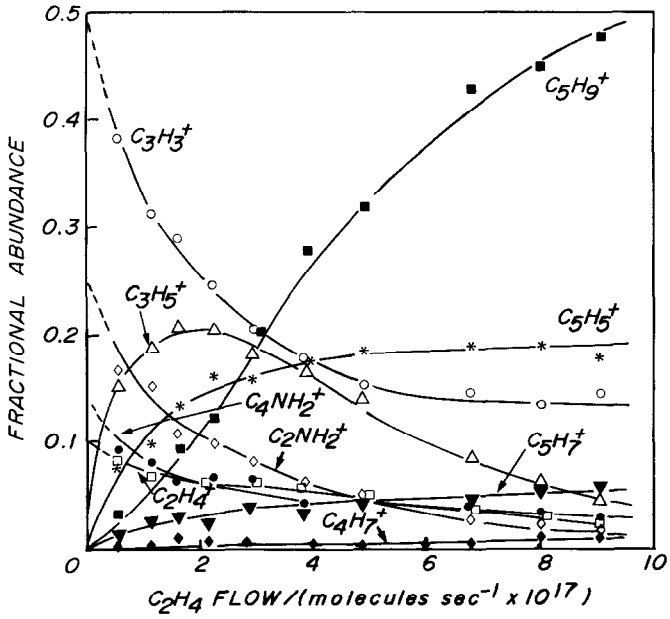

Fig. 3. Fractional abundance of the product ions observed for the reaction of C_2N^+ with ethylene as a function of the addition of ethylene. Deuterium has been added upstream to scavenge the higher-energy component. Helium buffer gas. $P = 0.40$ torr, $\bar{v} = 6.5 \times 10^3$ cm s^{-1}, $L = 46$ cm, and $T = 296$ K. The plot is useful for the analysis of products. For example, the intercepts at zero flow provide a measure of the branching ratios of the primary products (see ref. 19).

Secondary ions with masses corresponding to both of these ions were observed. The non-reactive fraction of the $C_3H_3^+$ shown in Fig. 3 can be attributed to the cyclopropenium isomer which is known not to react rapidly with ethylene [24].

The formation of $C_2H_2N^+$ and $C_4H_2N^+$ seems to involve H_2 abstraction and H_2 elimination, respectively, while the isomers of $C_3H_3^+$ are achieved presumably through C–H bond insertion with and without cyclization. Charge transfer makes only a minor contribution to the overall reaction.

The major secondary ion appeared at $m/z = 41$, which is presumably $C_3H_5^+$ and not $C_2H_3N^+$. The former ion is likely to be produced by the secondary reactions

$$C_2H_2N^+ + C_2H_4 \rightarrow C_3H_5^+ + HCN \tag{14a}$$

$$C_4H_2N^+ + C_2H_4 \rightarrow C_3H_5^+ + HC_3N \tag{14b}$$

$C_2H_4^+$ is known to produce $C_3H_5^+$ and $C_4H_7^+$ with ethylene [25]. The latter ion was also observed as a secondary product. The reaction of $C_4H_2N^+$ may

also contribute to the formation of the ion at $m/z = 65$ as indicated in the reaction

$$C_4H_2N^+ + C_2H_4 \rightarrow C_5H_5^+ + HCN \quad (15)$$

The major tertiary product ion was observed at $m/z = 69$, which is likely to be $C_5H_9^+$ formed by the known association reaction of $C_3H_5^+$ with ethylene [26].

The same four primary product ions were reported for the ICR measurements [12] and the agreement between the rate constants obtained in the ICR and SIFT studies is within experimental error. However, the two main product channels reported in the ICR studies are inverted in relative importance to that obtained in the SIFT measurements.

H_2S

Upstream addition of oxygen did not noticeably influence the decay of C_2N^+ observed with the addition of hydrogen sulphide downstream. The reaction was rapid with and without scavenger gas, $k = 1.2 \times 10^{-9}$ cm^3 molecule^{-1} s^{-1}. With added oxygen, HCS^+ was the predominant product ion and C_2NS^+ a significant minor product. The former product ion may be achieved by S–H bond insertion, while the latter will result from S-atom abstraction. There was evidence for some ($\leq 5\%$) production of H_2S^+ and CH_2N^+ but the H_2S^+ could be accounted for by the charge transfer with the O_2^+ initially present under these conditions. No further reactions were observed with HCS^+, C_2NS^+, and C_2NO^+, $k \leq 2 \times 10^{-12}$ cm^3 molecule^{-1} s^{-1}. Removal of oxygen appeared to enhance the relative production of C_2NS^+, CH_2N^+, and H_2S^+.

NH_3

Only one slope was associated with the decay observed for the reaction of C_2N^+ with ammonia. The addition of oxygen did not influence this decay, which was fitted with an average rate constant of 1.8×10^{-9} cm^3 molecule^{-1} s^{-1}. The major product ion with and without oxygen was CH_2N^+, which reacted further with ammonia to produce NH_4^+. The ions NH_3^+ and HN_2^+ were also observed in the product spectrum but with a minor contribution to the total products ($\leq 10\%$). They were observed with and without oxygen and both of them reacted further with ammonia to produce NH_4^+. In the presence of oxgen, the known charge transfer reaction with O_2^+ contributes to the formation of NH_3^+ so that the contribution of charge transfer to the

reaction of CNC^+ could not be established with high confidence. The formation of CH_2N^+ and HN_2^+ according to the reactions

$$C_2N^+ + NH_3 \rightarrow CH_2N^+ + CHN \quad (16a)$$

$$\rightarrow HN_2^+ + C_2H_2 \quad (16b)$$

is exothermic for both isomers. C_2NO^+ was observed to react with ammonia. The products could not be identified unequivocally, but CH_2N^+ and CHNO are the most likely.

CS_2

The predominant channel observed with carbon disulphide was S-atom abstraction to produce C_2NS^+. The presence of oxygen did not influence the specific reaction rate, $k = 9.2 \times 10^{-10}$ cm^3 molecule^{-1} s^{-1}. There was evidence for some charge transfer with the reactive component as CS_2^+ was observed to increase in the absence of oxygen. In the presence of oxygen, the increase in the CS_2^+ ion was less and could be accounted for by charge transfer to the O_2^+ ion initially present under these conditions. No reactions were observed with the ions C_2NO^+ and C_2NS^+, $k \leq 1 \times 10^{-11}$ cm^3 molecule^{-1} s^{-1}.

NO

Charge transfer was the only significant channel observed for the reaction of C_2N^+ with nitric oxide. The specific reaction rate was 6.2×10^{-10} cm^3 molecule^{-1} s^{-1} and it was found to be independent of the presence of the scavenger gas. The experiments in the absence of oxygen allowed an upper limit of 1% to be set on the production of C_2NO^+ from either isomer of C_2N^+. The C_2NO^+ formed upstream in the presence of oxygen was unreactive towards NO, $k \leq 2 \times 10^{-12}$ cm^3 molecule^{-1} s^{-1}.

CONCLUSIONS

The observed reactions of C_2N^+ derived from cyanogen by electron impact show an interesting range in reactivity. The experimental evidence for two components of C_2N^+ of different reactivity is unambiguous. One component reacts exclusively with H_2, D_2, CO_2, Xe, and O_2. This reactive component can be identified as the CCN^+ isomer on the basis of the enthalpies of formation available for the CCN^+ and CNC^+ isomers and the observation of the reaction with H_2, which produces CH_2N^+. The reaction with H_2 is exothermic only with the higher-energy CCN^+ isomer and only to produce the lowest-energy isomer of CH_2N^+, viz. protonated at the N end.

The C_2N^+ established with the addition of O_2, H_2, or D_2 scavenger gas upstream in the flow tube shows a reactivity consonant with that expected for the lower-energy CNC^+ isomer. The measured rate constants and product distributions are consistent with the results of our earlier SIFT experiments in which C_2N^+ was produced chemically by reaction (1) and reacted with H_2, H_2O, CH_4, CH_3CN, C_2H_2, H_2S, and NH_3 [11]. Reaction (1) has been shown by the recent crossed-beam study to lead to the more stable CNC^+ isomer at low relative energies [13]. The available enthalpies of formation indicate that the production of the higher energy CCN^+ isomer by reaction (1) is endothermic by 2 ± 4 kcal mol^{-1}. Of the six reactions investigated in the earlier SIFT studies, the reactions with H_2, H_2O, and CH_4 are most sensitive to the isomeric identity of C_2N^+. It is evident from the measured rate constants for these three reactions that the C_2N^+ produced chemically by reaction (1) is the same as the fraction of the C_2N^+ generated from cyanogen by electron impact, which was identified as the lower energy CNC^+ isomer.

The reactivities observed for the lower-energy component are also reasonably consistent with the reactivities reported in the recent ICR study in which C_2N^+ was derived from cyanogen by electron impact at 19.5 eV, although these had been tentatively ascribed to the higher-energy isomer [12]. The measured reactions which are common to the earlier ICR and the present SIFT studies are those with N_2, CO, HCN, CO_2, C_2N_2, H_2O, CH_4, C_2H_2, C_2H_4, and NH_3. Of these, only the reactions with CO_2, H_2O, and CH_4 were observed in the SIFT study to be sensitive to the identity of the C_2N^+. All three were found to be rapid with CCN^+ and slower or non-observable with CNC^+. The ICR experiments showed no reaction with CH_4 and CO_2, $k \leq 1 \times 10^{-11}$ cm^3 $molecule^{-1}$ s^{-1}, and a reaction with H_2O with a rate constant consistent with that obtained in the SIFT study for CNC^+. The CNC^+ isomer also was seen in the SIFT study to react slowly with methane with a rate constant below the measurable limit indicated in the ICR study, 3.9×10^{-12} vs. 1×10^{-11} cm^3 $molecule^{-1}$ s^{-1}, and not at all with CO_2, $k \leq 3 \times 10^{-14}$ cm^3 $molecule^{-1}$ s^{-1}. These results provide a convincing case for the production of the CNC^+ isomer in the ICR experiments rather than the CCN^+ isomer as had been suggested earlier [12]. There are some differences in the product distributions observed in the ICR and SIFT experiments for the reactions with NH_3, H_2O, C_2H_2, and C_2H_4, which were addressed in the discussion of results but these can be considered, for the most part, to be minor. Furthermore, there is agreement between the ICR and SIFT results in the rate constants obtained for the reactions with N_2, CO, C_2H_2, C_2H_4, and NH_3. There is also agreement for the reactions with HCN and C_2N_2, which were observed to proceed rapidly by association at the pressures of the SIFT experiments and not observed at

all at the low pressures of the ICR experiments, as would be expected if the association occurs in a termolecular fashion.

Many of the observed reaction channels are in accord with a carbenoid character for the two isomers of C_2N^+ as was the case for the reaction channels identified recently in an extensive study of the chemistry of the carbene cation $:C_3H^+$ [14]. In fact, there is a remarkable correspondence between the results obtained for the reactions of C_2N^+ and C_3H^+. The carbene character of the two isomers of C_2N^+ is evident from the Lewis formulas

$:N{\equiv}C{-}C^+: \leftrightarrow {}^+{:}N{=}C{=}C:$

$:C{=}\ddot{N}{-}C^+: \leftrightarrow :C{=}N^+{=}C:$

Co-ordination with a non-bonded electron pair on oxygen in N_2O and CH_3OH for the reactions of CNC^+ and also CO_2, H_2O, O_2, and OCS for the reactions of CCN^+ can account for the product ion C_2NO^+ observed with these reagents. Similarly, co-ordination with a non-bonded electron pair on sulphur in OCS, H_2S, and CS_2 can account for the product ion C_2NS^+.

Insertion can account for several of the product channels observed with the molecules containing C–H, N–H, O–H, or S–H bonds, in particular the channels leading to the formation of CHN or CH_2N^+. Also, it appears that the formation of the adducts observed with H_2, HCN, and C_2N_2 may involve sigma-bond insertion. Nitride ion transfer occurs with N_2O, as was the case with C_3H^+ [14]. It is interesting to note in this case that different isomers of C_2N_2 can be expected to be formed from the two different isomers of C_2N^+, viz. $:CCN^+$ is likely to produce $N{\equiv}C{-}C{\equiv}N$, while $:CN^+C:$ is likely to produce $:C{=}N{-}C{\equiv}N$. The $C_3H_2N^+$ product ion observed with methane and methanol appears to involve the addition of methylene to the C_2N^+. The two different isomers of C_2N^+ can lead to two different isomers of $C_3H_2N^+$, viz. $:CCN^+$ can lead to $H_2C{=}C^+{-}C{\equiv}N$ and $:CN^+C:$ can lead to $:C{=}N{-}C^+{=}CH_2$.

The observed charge transfer reaction with Xe^+ places the recombination energy of CCN^+ above or just slightly below the ionization energy of Xe, IP(Xe) = 12.130 eV. The latter possibility arises because of the low reaction efficiency observed for charge transfer reaction, $k/k_c = 0.03$, which may mean that the charge transfer reaction is slightly endothermic. The CCN^+ reacts by oxygen-atom transfer with the molecules CO_2, N_2O, H_2O, O_2, and CH_3OH but the structure of the product ion C_2NO^+ is uncertain. Both $CCNO^+$ and $OCCN^+$ are possible and both are resonance stabilized

$:C{=}C^+{-}N{=}O \leftrightarrow :C{=}C{=}N{-}O^+$

$O{=}C{=}C{=}N^+ \leftrightarrow O{=}C^+{-}C{\equiv}N$

Molecular orbital calculations have indicated that the $OCCN^+$ isomer has an enthalpy of formation of 278 ± 10 kcal mol^{-1} and is more stable than the $CCNO^+$ isomer by 130 kcal mol^{-1} [27]. The absolute value for the enthalpy of formation is consistent with the experimental observations. The oxygen-atom abstraction reaction observed with OCS places an upper limit of 314 kcal mol^{-1} to the enthalpy of formation of the C_2NO^+ produced in this reaction, while the failure to observe oxygen-atom transfer with CO implies a lower limit of 215 kcal mol^{-1}. The CNC^+ isomer also produces C_2NO^+ but only with N_2O and CH_3OH. The structure of this ion should be $CNCO^+$ and so is different from the structure of the C_2NO^+ produced from the CCN^+ isomer. The observation of the oxygen-atom abstraction reaction of CNC^+ with CH_3OH provides an upper limit to the enthalpy of formation for $CNCO^+$ of 357 kcal mol^{-1}. The molecular orbital calculations have indicated an enthalpy of formation of approximately 290 kcal mol^{-1} [27].

The C_2NO^+ ion derived from the reaction of CCN^+ with O_2, presumably the $OCCN^+$ isomer, was found to be quite unreactive. It was observed to react rapidly to form bimolecular products only with ammonia.

C_2N^+ is produced in interstellar gas clouds by the reaction of C^+ with HCN. It now seems certain from laboratory measurements that the CNC^+ isomer is the exclusive product when these reactants are in their ground states. Since CNC^+ is unreactive towards H_2 and CO, which are the main molecular gases in these clouds, it becomes available for reactions with the minor gaseous constituents. The results reported here provide insight into some likely consequences. We have suggested previously that the reaction of C^+ with HCN does not constitute a major loss process with HCN since many of the reactions of C_2N^+ appear to recycle the HCN consumed in its formation, as is illustrated in the reaction sequence [11]

$$C^+ + HCN \rightarrow CNC^+ + H \tag{17a}$$

$$CNC^+ + HX \rightarrow CX^+ + CHN \tag{17b}$$

Reactions of type (17b) have now been observed with H_2O, H_2S, NH_3, C_2H_2, CH_4, C_2H_4, and CH_3OH. We should note here, however, that the structure of neutral product CHN is uncertain. Reactions of type (17b) may well lead to the formation of CNH rather than HCN, in which case they would provide a means for the isomerization of HCN. Reaction channels other than (17b), and the related channel involving intramolecular proton transfer, do represent loss processes for HCN, as does the reaction of CNC^+ with HCN itself if it proceeds by radiative association.

The reactions of type (17b) lead to C–X bond formation in analogy with the counterpart reactions involving C^+. Thus C–O, C–S, and C–N bond formation occur with H_2O, H_2S, and NH_3, respectively, while C–C bond

formation occurs with C_2H_2, CH_4, C_2H_4, and probably CH_3OH. Neutralization of the CX^+ ions formed in these reactions will lead to the formation of CO, CS, CHN, C_3, C_2H_2, C_3H_2, and C_2H_2O. Various isomers are possible for CHN, C_2H_2, C_3H_2, and C_2H_2O. For example, H–X insertion followed by elimination of CHN and neutralization of $C–X^+$ (where X = NH_2, CH_3, $CHCH_2$) may lead to :CNH, :C=CH_2, :C=C=CH_2, and c-:C_3H_2. Together with the formation of :CO, :CS, and :C=C=C:, this chemistry is directed towards the synthesis of carbenes in interstellar gas clouds [28].

Some other specific reactions of CNC^+ are also of interest with regard to the growth of molecules in interstellar clouds. The very rapid reaction with CH_3CN is a direct source for cyanogen, or possibly isocyanogen :C=N–C≡N. If the rapid association reactions with HCN and C_2N_2 occur radiatively in intersellar gas clouds, they may provide routes toward :$C(CN)_2$ and $C(CN)_3$. Reactions with OCS, H_2S, and CS_2 may lead to CNCS when C_2NS^+ is neutralized by charge transfer. The methylene abstraction reaction with methane which is proposed to lead to :C=N–C^+=CH_2 would be a source of isocyano-acetylene. This molecule may also be formed in the neutralization of the $C_3H_2N^+$ ion produced from methanol. The reaction of CNC^+ with methanol is also a possible source of :C(NC:)OH since C_2HNO is formed directly along with CH_3^+. Finally, the reaction with ethylene which produces $C_4H_2N^+$ and the two isomers of $C_3H_3^+$ is a possible source for :C(N=C:)CCH, :C=C=CH_2, and the cyclic carbene :C_3H_2.

ACKNOWLEDGEMENT

We thank the Natural Sciences and Engineering Research Council of Canada for financial support.

REFERENCES

1 T.W. Hartquist and A. Dalgarno, in P.M. Solomon and M.G. Edmunds (Eds.), Giant Molecular Clouds in the Galaxy, Pergamon Press, London, 1980, p. 315.
2 G.F. Mitchell, J.L. Ginsberg and P.J. Kuntz, Astrophys. J. Suppl., 38 (1978) 39.
3 H.I. Schiff and D.K. Bohme, Astrophys. J., 232 (1979) 740.
4 V.G. Anicich, W.T. Huntress and J.H. Futrell, Chem. Phys. Lett., 40 (1976) 233.
5 J.P. Liddy, C.G. Freeman and M.J. McEwan, Mon. Not. R. Astron. Soc., 180 (1977) 683.
6 D.C. Clary, D. Smith and N.G. Adams, Chem. Phys. Lett., 119 (1985) 320.
7 N.N. Haese and R.C. Woods, Astrophys. J., 246 (1981) L51.
8 P.W. Harland and B.J. McIntosh, Int. J. Mass Spectrom. Ion Processes, 67 (1985) 29.
9 P.W. Harland, Int. J. Mass Spectrom. Ion Processes, 70 (1986) 231.
10 M. Yoshimine and W.P. Kraemer, Chem. Phys. Lett., 90 (1982) 145.
11 H.I. Schiff, G.I. Mackay, G.D. Vlachos and D.K. Bohme, in B. Andrews (Ed.), Proc. I.A.U. Symp. Interstellar Molecules, No. 87, Reidel, Dordrecht, 1981, p. 307.

12 M.J. McEwan, V.G. Anicich, W.T. Huntress, P.R. Kemper and M.T. Bowers, Int. J. Mass Spectrom. Ion Phys., 50 (1983) 179.
13 R.G. Daniel, E.R. Keim and J.M. Farrar, Astrophys. J., 303 (1986) 439.
14 A.B. Raksit and D.K. Bohme, Int. J. Mass Spectrom. Ion Processes, 55 (1984) 69.
15 G.I. Mackay, G.D. Vlachos, D.K. Bohme and H.I. Schiff, Int. J. Mass Spectrom. Ion Phys., 36 (1980) 259.
16 Extranuclear Laboratories, Pittsburgh, PA 15238, U.S.A., Model 0413.
17 O. Glemser, in G. Brauer (Ed.), The Handbook of Preparative Inorganic Chemistry, Academic Press, New York, 1963, p. 658.
18 J. Glosik, A.B. Raksit, D.G. Lister, N.D. Twiddy, N.G. Adams and D. Smith, J. Phys. B, 11 (1978) 3365.
19 N.G. Adams and D. Smith, J. Phys. B, 9 (1976) 1439.
20 C.G. Freeman, P.W. Harland and M.J. McEwan, Aust. J. Chem., 31 (1978) 963.
21 D.K. Bohme, S. Dheandhanoo, S. Włodek and A.B. Raksit, J. Phys. Chem., 91 (1987) 2569.
22 A.B. Raksit and D.K. Bohme, Int. J. Mass Spectrom. Ion Processes, 55 (1985) 217.
23 J.M. Van Doren, S.E. Barlow, C.H. DePuy, V.M. Bierbaum, I. Dotan and E.E. Ferguson, 90 (1986) 2772.
24 K.C. Smyth, S.G. Lias and P. Ausloos, Combust. Sci. Technol., 28 (1982) 147.
25 J.K. Kim, V.G. Anicich and W.T. Huntress, J. Phys. Chem., 81 (1977) 1978.
26 J.A. Burt, J.L. Dunn, M.J. McEwan, M.M. Sutton, A.E. Roche and H.I. Schiff, J. Chem. Phys., 52 (1970) 6062.
27 M.H. Lien and A.C. Hopkinson, unpublished results. The enthalpy of formation of $OCCN^+$ is based on the energy of its dissociation into CO and CN^+ (4π electrons). This energy and the relative energy of $OCCN^+$ and $CNCO^+$ were calculated at the level MP4SDTQ/6-31G*//6-31G*. The relative energy of $OCCN^+$ and $CCNO^+$ was calculated at the HF 6-31G* level.
28 D.K. Bohme, Nature (London), 319 (1986) 473.
29 T. Su and W.J. Chesnavich, J. Chem. Phys., 76 (1982) 5183.